Title

Extracting a History of Global Fire Emissions for the Past Millennium From Ice Core Records of Acetylene, Ethane, and Methane

Journal

Journal of Geophysical Research: Atmospheres, 125(20)

ISSN

2169-897X

Authors

Nicewonger, Melinda R
Aydin, Murat
Prather, Michael J
et al.

Publication Date

2020-10-27

DOI

10.1029/2020jd032932

Peer reviewed

JGR Atmospheres

RESEARCH ARTICLE
10.1029/2020JD032932

Extracting a History of Global Fire Emissions for the Past Millennium From Ice Core Records of Acetylene, Ethane, and Methane

Melinda R. Nicewonger[1], Murat Aydin[1], Michael J. Prather[1], and Eric S. Saltzman[1,2]

[1]Department of Earth System Science, University of California, Irvine, CA, USA, [2]Department of Chemistry, University of California, Irvine, CA, USA

Key Points:
- Paleofire trends inferred from ice core acetylene, ethane, and methane isotopes are shown to be consistent for the past millennium
- The trace gas records do not yield a quantitatively consistent fire history even assuming dramatic changes to the location of fires
- Major changes in atmospheric lifetime or transport are required to reconcile the burning histories inferred from the three trace gases

Supporting Information:
- Supporting information S1

Correspondence to:
M. R. Nicewonger,
nicewonm@uci.edu

Citation:
Nicewonger, M. R., Aydin, M., Prather, M. J., & Saltzman, E. S. (2020). Extracting a history of global fire emissions for the past millennium from ice core records of acetylene, ethane, and methane. *Journal of Geophysical Research: Atmospheres*, *125*, e2020JD032932. https://doi.org/10.1029/2020JD032932

Received 15 APR 2020
Accepted 29 SEP 2020
Accepted article online 5 OCT 2020

Author Contributions:
Conceptualization: Melinda R. Nicewonger, Eric S. Saltzman
Data curation: Murat Aydin, Eric S. Saltzman
Formal analysis: Melinda R. Nicewonger, Michael J. Prather
Funding acquisition: Murat Aydin, Eric S. Saltzman
Investigation: Melinda R. Nicewonger
Methodology: Melinda R. Nicewonger, Murat Aydin
Resources: Michael J. Prather, Eric S. Saltzman
Software: Michael J. Prather
Supervision: Murat Aydin, Eric S. Saltzman
Writing - original draft: Melinda R. Nicewonger
(continued)

Abstract Biomass burning is an important component of the Earth system in terms of global biogeochemistry, atmospheric composition, climate, terrestrial ecology, and land use. This study examines published ice core trace gas measurements of acetylene, ethane, and methane, which have been used as proxies for paleofire emissions. We investigate the consistency of these records for the past 1,000 years in terms of (1) temporal trends in global fire emissions and (2) quantitative estimates for changes in global burning (dry matter burned per year). Three-dimensional transport and box models were used to construct emissions scenarios for the trace gases consistent with each ice core record. Burning histories were inferred from trace gas emissions by accounting for biome-specific emission factors for each trace gas. The temporal trends in fire inferred from the trace gases are in reasonable agreement, with a large decline in biomass burning emissions from the Medieval Period (MP: 1000–1500 CE) to the Little Ice Age (LIA: 1650–1750 CE). However, the three trace gas ice core records do not yield a consistent fire history, even assuming dramatic (and unrealistic) changes in the spatial distribution of fire and biomes. Substantial changes in other factors such as meteorological transport or atmospheric photochemical lifetimes appear to be required to reconcile the trace gas records.

Plain Language Summary Biomass burning (wildfires) are an important component of the climate system. Understanding how biomass burning has changed in the past can help us better predict how biomass burning may change in the future. This study examines ice core measurements of three trace gases, acetylene, ethane, and methane, in order to determine if a single global "fire history" (dry matter burned) can be reconstructed over the last 1,000 years. All three ice core records indicate a large decline in their respective biomass burning emissions after 1500 CE. However, a single fire history of dry matter burned over the last 1,000 years is not easily reconstructed from the ice core records even when enacting extreme changes to the location of fires and biome types. This suggests that our knowledge of the preindustrial fire system is incomplete. There appears to be little doubt that large changes occurred in biomass burning over the past millennium, although the exact magnitude and location of those changes are not yet quantifiable.

1. Introduction

Fires are a major source of carbon-containing gases to the atmosphere, including the greenhouse gases carbon dioxide and methane (Akagi et al., 2011; Andreae & Merlet, 2001). Fires also impact climate through emissions of aerosols and photochemically reactive gases, like black carbon and carbon monoxide. There is debate about past variability in global burning and the extent to which humans have changed the natural fire system (Andela et al., 2017; Archibald et al., 2009; Bowman et al., 2009, 2011; Hantson et al., 2016; van Marle et al., 2017). A quantitative knowledge of the variability in past burning may help us assess past climate forcing from fire and improve our understanding of the climate/fire relationship on centennial and millennial time scales (Hantson et al., 2016; Solomon et al., 2007; van der Werf et al., 2013; van Marle et al., 2017). Many different metrics are used to assess fire activity, such as fire extent, frequency, and severity (Andela et al., 2017; Marlon et al., 2008, 2013, 2016; Power et al., 2008, 2012; van der Werf et al., 2006, 2010, 2017). In this study, we focus specifically on pyrogenic emissions of trace gases and global burning (Pg dry matter burned per year).

Writing – review & editing: Melinda R. Nicewonger, Murat Aydin, Eric S. Saltzman

Biomass burning records for the past millennium have been developed from sedimentary charcoal and impurities in ice cores (e.g., Bock et al., 2017; Ferretti et al., 2005; Grieman et al., 2017; Grieman, Aydin, Isaksson, et al., 2018; Grieman, Aydin, McConnell, et al., 2018; Kawamura et al., 2012; Kehrwald et al., 2012; Legrand et al., 1992, 2016; Marlon et al., 2008; McConnell et al., 2007; Power et al., 2008, 2012; Rubino et al., 2015; Simoneit et al., 1999). The global charcoal record indicates a decline in burning activity from 1000–1750 CE, reaching a minimum during the Little Ice Age period followed by a sharp rise from 1750–1870 CE and a decline into the twentieth century (Figure 1; Marlon et al., 2008). The global charcoal database is a record of fire activity, rather than a direct measure of fire emissions. Reconstructing emissions from charcoal records would require considering known biases such as the underrepresentation of fires in grassland/dry shrubland biomes where low woody biomass limits charcoal production (Marlon et al., 2008). This biome accounts for over half of the modern-day carbon emission from fires (van der Werf et al., 2017).

Ice core trace gas measurements of methane and $\delta^{13}CH_4$, ethane, acetylene, and carbon monoxide also have been used to reconstruct trends in global fire emissions over the past millennium (Figure 2) (Bock et al., 2017; Ferretti et al., 2005; Mischler et al., 2009; Nicewonger et al., 2016, 2018, 2020; Sapart et al., 2012; Wang et al., 2010). Methane has an 8- to 10-year atmospheric lifetime and therefore the potential to provide a globally integrated signal of pyrogenic emissions. Ferretti et al. (2005) interpreted the methane isotope records over the past millennium as indicating a complexity of the methane and methane isotope budgets. Interpretation of the methane isotope signal in terms of pyrogenic emissions requires assumptions about trends in microbial emissions and knowledge of the end-member isotopic composition of multiple sources.

Acetylene has a simple biogeochemical cycle, with fire as the major source during the preindustrial (see section 2.1 for global budget discussions) (Nicewonger et al., 2020; Xiao et al., 2007). Ethane has one additional source from geologic emissions, the magnitude of which is controversial (Dyonisius et al., 2020; Etiope & Ciccioli, 2009; Hmiel et al., 2020; Petrenko et al., 2017). Methane and CO are considerably more complex. Microbial sources comprise most of the preindustrial CH_4 emissions with geologic emissions as another possible, but debated source (Dyonisius et al., 2020; Etiope & Ciccioli, 2009; Hmiel et al., 2020; Petrenko et al., 2017). CO has preindustrial sources from biomass burning and from atmospheric oxidation of methane and nonmethane hydrocarbons. To obtain a history of biomass burning from ice core CO and CH_4, co-measurements of the stable isotopic composition of CH_4 and CO are required to partition the biomass burning source from their other sources (Bock et al., 2017; Ferretti et al., 2005; Mischler et al., 2009; Sapart et al., 2012; Wang et al., 2010). Uncertainties in the value of the isotopic source magnitudes through time ultimately leads to challenges interpreting the CO and CH_4 data and may explain some of the differences between trends in different ice core proxy records (Sowers, 2010) (Figure 1).

Nicewonger et al. (2020) demonstrated that the ice core acetylene, ethane, and methane biomass burning records have consistent temporal trends over the last 1,000 years with higher burning emissions during the 1000–1500 CE period (hereafter referred to as the Medieval Period, MP) followed by a sharp decline around 1500 CE into the Little Ice Age (LIA; 1650–1750 CE). Limited knowledge of the fossil fuel source magnitudes of acetylene and ethane after industrialization makes estimating the biomass burning source of these gases into the modern era highly uncertain (Nicewonger et al., 2018, 2020). However, qualitatively, the ice cores levels of acetylene and ethane do not show any large changes into the mid-1800s from their mean level in the 1700s, indicating that the sources, including biomass burning, likely stayed low through the end of the nineteenth century (Figure 2) (Nicewonger et al., 2018, 2020). In contrast, the CO ice core record indicates increased biomass burning emissions around the late-1800s, consistent with the temporal trends found in the charcoal proxy record. The exact cause of the differences between the ice core acetylene, ethane, and methane records with the CO record has not yet be determined (Nicewonger et al., 2018, 2020) and until co-measurements of all these gases are made in the same ice core, it may be challenging to resolve.

Here we focus on comparing the ice core acetylene, ethane, and methane records to determine if all three gases are consistent with a single fire history (dry matter burned per year) for the past 1,000 years. We utilize a base case in which the spatial/seasonal distribution of biomass burning and emission factors are fixed at their modern values (Global Fire Emissions Database Version 4, GFED4; van der Werf et al., 2017). There is abundant evidence to suggest the location of fires has changed over the past 1,000 years (e.g., Marlon et al., 2008; Power et al., 2012). The impact of such changes are explored in additional scenarios. Other

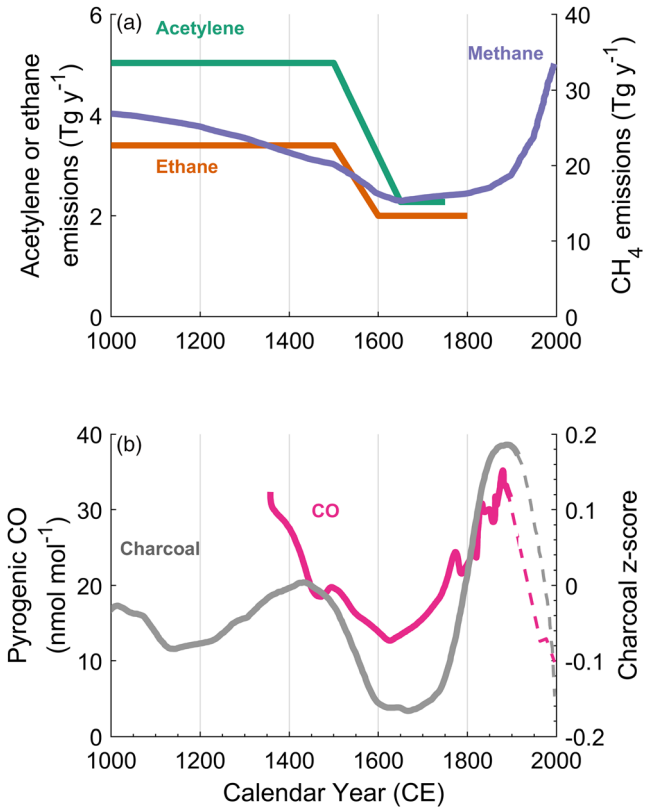

Figure 1. Biomass burning proxies from ice core gases and from global charcoal for the past 1,000 years. (a) Inferred biomass burning emissions from ice core acetylene (green; Nicewonger et al., 2020), ethane (orange; Nicewonger et al., 2018), and methane and $\delta^{13}CH_4$ (purple; Ferretti et al., 2005). (b) Inferred biomass burning emissions from carbon monoxide and its isotopes (pink; Wang et al., 2010) and global fire activity from global charcoal (Marlon et al., 2008).

issues considered include the possible impact of changes in atmospheric lifetime of ethane and methane due to chlorine atoms, variability in the isotopic signatures of methane sources, and changes in trace gas emission factors.

2. Atmospheric Cycling and Budgets of Acetylene, Ethane, and Methane

2.1. Acetylene

Acetylene is released from incomplete combustion processes, including fossil fuel and biofuel burning and biomass burning (Whitby & Altwicker, 1978; Xiao et al., 2007). The global acetylene budget is estimated at roughly 7 Tg year^{-1} with about half of the emissions from biofuel burning and the remaining half split equally between fossil fuel and biomass burning (Xiao et al., 2007). Acetylene may also have a small source from partial combustion of methane through geologic outgassing (i.e., mud volcanoes) (Anderson, 1958; Gunter & Musgrave, 1971; Liu et al., 2017). This source is not well quantified but is likely to be a minor component of the budget (Nicewonger et al., 2020). Acetylene is lost in the atmosphere via reaction with the hydroxyl radical, resulting in a global mean lifetime of roughly 2–3 weeks (Burkholder et al., 2015; Xiao et al., 2007). A minor sink to chlorine atoms also occurs, but this sink accounts for less than 1% of the total loss (Burkholder et al., 2015; Wang et al., 2019) and therefore does not contribute significantly to variability in atmospheric acetylene levels. Acetylene is an ideal proxy for paleobiomass burning because the biomass burning source is believed to be the only major source of acetylene to the preindustrial atmosphere (Nicewonger et al., 2020). The ice core records of acetylene from Greenland and Antarctica are shown in Figure 2.

2.2. Ethane

Ethane is emitted to the modern atmosphere primarily from the production, processing, transmission and use of oil and natural gas, burning of biofuels and biomass, and natural geologic seeps (Etiope & Ciccioli, 2009; Helmig et al., 2016; Pozzer et al., 2010; Rudolph, 1995; Simpson et al., 2012; Tzompa-Sosa et al., 2017; Xiao et al., 2008). Minor emissions from oceanic and terrestrial ecosystems have been suggested but are highly uncertain (Clarkson et al., 1997; Plass-Dülmer et al., 1995; Stein & Rudolph, 2007). Total global emissions of ethane have been estimated at 10–20 Tg year^{-1} with roughly two thirds of the budget from human use of fossil fuels and biofuels (Aydin et al., 2011; Dalsøren et al., 2018; Etiope & Ciccioli, 2009; Franco et al., 2016; Helmig et al., 2016; Nicewonger et al., 2016; Rudolph, 1995; Simpson et al., 2012; Tzompa-Sosa et al., 2017; Xiao et al., 2008). The largest natural source of ethane is from biomass burning emissions with global emissions around 3.4 Tg year^{-1} during the satellite era (1997–2017) (Giglio et al., 2013; van der Werf et al., 2017). Geologic ethane emissions in the modern atmosphere are estimated at 2–4 Tg year^{-1} (Etiope & Ciccioli, 2009). However, the importance and magnitude of geologic hydrocarbons in the preindustrial atmosphere has been heavily debated based on measurements of radiocarbon-free methane in ice cores (Dyonisius et al., 2020; Hmiel et al., 2020; Petrenko et al., 2017).

The major sink of atmospheric ethane is via oxidation with the hydroxyl radical (OH) resulting in a global mean lifetime of roughly 2 months (Burkholder et al., 2015; Poisson et al., 2000; Rudolph, 1995; Xiao et al., 2008). Ethane is also oxidized by chlorine atoms which are produced in the marine boundary layer by reactions involving marine aerosols and polluted air (Knipping & Dabdub, 2003; Lawler et al., 2009; Wang et al., 2019). The reaction rate constant with chlorine occurs at a rate roughly 230 times faster than the reaction rate constant with OH (Burkholder et al., 2015). This reaction has been omitted from most budget analyses of ethane (e.g., Pozzer et al., 2010; Tzompa-Sosa et al., 2017; Xiao et al., 2008) because the distribution and magnitude of chlorine atoms is not well known. Recent analysis by Wang et al. (2019) shows

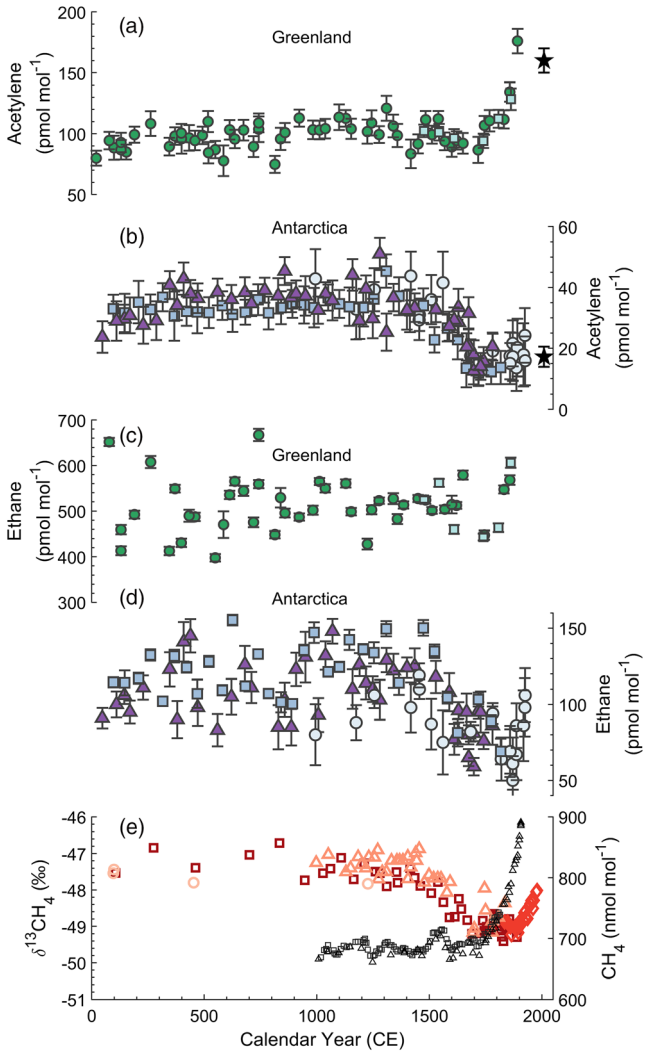

Figure 2. Ice core acetylene, ethane, methane, and $\delta^{13}CH_4$ over the last 2,000 years. (a) Greenland ice core acetylene (Nicewonger et al., 2020) from GISP2B (squares) and GISP2D (circles) and the present-day atmospheric level over Greenland (star; Helmig, 2017), (b) Antarctic ice core acetylene (Nicewonger et al., 2020) from WDC05A (circles), WDC06A (triangles) and SPC14 (squares), and the present day atmospheric level over Antarctica (star) (c) same as in (a) but for ethane (Nicewonger et al., 2018) with additional data back to 0 CE (this study). (d) Same as in (b) but for ethane (Nicewonger et al., 2018) with additional data back to 0 CE (this study), (e) left: Ice core $\delta^{13}CH_4$ from the DSS, DE08 (squares, Ferretti et al., 2005), WDC05A (triangles, Mischler et al., 2009), and TALDICE (circles, Bock et al., 2017) ice cores; right: Antarctic ice core methane (in nmol mol^{-1}) from WDC05A (Mitchell et al., 2011) and Law Dome (Etheridge et al., 1998). Error bars on the acetylene and ethane measurements represent 1σ uncertainties.

the reaction with chlorine may constitute a significant portion (~20%) of the ethane sink. The ice core records of ethane from Greenland and Antarctica are shown in Figure 2.

2.3. Methane

Methane is emitted to the atmosphere through fossil fuel production, transport and use (including natural gas, coal, and oil), biomass and biofuel burning, geologic outgassing (seepage), and biogenic sources (e.g., wetlands, ruminant animals, agriculture and waste, and thawing permafrost) (Dlugokencky et al., 2011; Etiope, 2012; Kirschke et al., 2013; Nisbet et al., 2014). Roughly two-thirds of methane emissions today are from human activities. The main destruction of atmospheric methane occurs via oxidation with the hydroxyl radical (OH) resulting in an atmospheric lifetime of roughly 9–10 years (Dlugokencky et al., 2011; Kirschke et al., 2013; Prather et al., 2012). Methane is also lost by reaction with chlorine atoms. The magnitude of this sink term is not well constrained but is estimated in the range of 1–5% of the total loss (Allan et al., 2007; Prather et al., 2012; Wang et al., 2019).

Ice core measurements of the abundance of methane and its stable isotopic composition ($\delta^{13}CH_4$) have been used to reconstruct the preindustrial methane budget (Figure 2) (Beck et al., 2018; Bock et al., 2017; Ferretti et al., 2005; Mischler et al., 2009; Sapart et al., 2012). Inferring emissions from methane isotopic measurements and methane concentration requires knowledge of the isotopic end-member values for each source. These are known for the modern atmosphere (Schwietzke et al., 2016), but there may be climate or ecology induced changes in end-member values on centennial or millennial time scales (Sowers, 2010). Changes to the $\delta^{13}C$ of atmospheric CO_2 due to industrialization has also altered the isotopic values of the biogenic and biomass burning methane sources as plants are using more depleted $\delta^{13}C$ in their photosynthetic process, but these changes are well characterized (Rubino et al., 2013). The large kinetic isotope effect associated with reaction of CH_4 with chlorine atoms introduces another source of uncertainty in the preindustrial methane isotope budget that has not been addressed in previous studies (Ferretti et al., 2005; Lassey et al., 2007; Nicewonger et al., 2018).

The geologic outgassing of methane is a subject of current debate. Etiope and Schwietzke (2019) proposed that such emissions comprise 45 (27–63) Tg CH_4 year^{-1}, based on surface measurements from several hundred global sites. If constant, this would comprise roughly 20% of the preindustrial methane budget. Ice core $\Delta^{14}CH_4$ measurements indicate a much lower fraction of radiocarbon-depleted CH_4, with best estimates all less than 20 Tg year^{-1} (Dyonisius et al., 2020; Hmiel et al., 2020; Petrenko et al., 2017).

3. Methods

Here we describe the use of models to infer the biomass burning required to account for previously published ice core measurements of ethane (Nicewonger et al., 2018), acetylene (Nicewonger et al., 2020) and methane and $\delta^{13}CH_4$ (Bock et al., 2017; Ferretti et al., 2005; MacFarling Meure et al., 2006; Mischler et al., 2009; Mitchell et al., 2011; Sowers, 2010). For the short-lived gases, ethane and acetylene, a 3-D chemistry transport model was used to quantify how the levels of these gases over Greenland and Antarctica relate to emissions from different geographic footprints (section 3.1). For the longer-lived gas, methane, a one-box global atmospheric

model is used to estimate the global methane mixing ratio and $\delta^{13}CH_4$ isotopic signature for various emission scenarios (section 3.2). Using the ice core levels as a constraint, we estimate the emissions of the trace gases under various scenarios. A discussion of how emission scenarios were evaluated is described in section 3.3. Scenarios exploring changes in atmospheric lifetime due to the presence of chlorine atoms are also described (section 3.4).

3.1. Modeling: Chemistry Transport Model

The UCI-Chemistry Transport Model (UCI-CTM) is a 3-D tropospheric CTM (Holmes et al., 2013; Prather & Hsu, 2010). It was run with roughly 2.8° horizontal resolution and 57 vertical layers. Transport was driven by the European Center for Medium-Range Weather Forecasts (ECMWF) reanalysis-forecast meteorological fields, using tropospheric chemistry described by Holmes et al. (2013). Fossil fuel emissions of acetylene and ethane were based on the Representative Concentration Pathway (RCP) year 2000 inventories (Lamarque et al., 2010). Biomass burning emissions of dry matter were based on the Global Fire Emissions Database Version 3.1 (GFED3.1; van der Werf et al., 2010). Emission factors were used to calculate biomass burning emissions of acetylene and ethane from dry matter emissions (Akagi et al., 2011; Andreae, 2019).

Acetylene and ethane have atmospheric lifetimes comparable to or shorter than the characteristic transport times from their major sources to the polar regions. Consequently, transport and removal must be considered in order to estimate the variations in emissions responsible for atmospheric histories derived from ice core data. The UCI-CTM was used to estimate the sensitivity (defined as pmol mol^{-1} per Tg $year^{-1}$ emission) of acetylene and ethane levels over Greenland and Antarctica to various sources (Nicewonger et al., 2018, 2020). Sensitivities were estimated by defining a reference model simulation of the modern atmosphere and adding acetylene-like and ethane-like tracer species (Nicewonger et al., 2018, 2020). These tracers react with the same OH lifetime and stratospheric loss rate as acetylene and ethane but do not affect the abundance of OH in the model. The use of tracer species for this purpose is appropriate, as acetylene and ethane are low-level trace gases that do not significantly impact tropospheric photochemistry (Prather, 1994). Based on observational constraints, the best estimate of methane lifetime due to OH oxidation is 11.2 years (Prather et al., 2012). The UCI-CTM is slightly more reactive, with an OH methane lifetime of 8.9 years. To compensate for the elevated reactivity of the model, the OH reaction coefficients for acetylene and ethane were reduced by 25% (see supporting information, SI).

Simulations were conducted for a 3-year period using meteorological fields from 2005–2007 and the final year (2007) was used to calculate annual average air mass weighted acetylene and ethane mole fractions. Sensitivities for acetylene and ethane over Greenland and Antarctica were calculated as follows:

$$\text{Sensitivity} = \frac{\text{abundance over polar region}}{\text{emissions}} \quad (1)$$

in units of pmol mol^{-1}/Tg $year^{-1}$. Acetylene and ethane levels were calculated from model output by integrating the mass of each compound and the mass of air from the surface to roughly 500 hPa over the polar regions (60–90°N for Greenland and 60–90°S for Antarctica). Acetylene levels in each high latitude region are relatively uniform, consistent with global chemistry transport modeling (Nicewonger et al., 2020). Therefore, using the average mixing ratios in these regions is representative of the average mixing ratios over Greenland and Antarctica. Sensitivities were computed for emissions from biomass burning (from several different regions), biofuels, fossil fuels, and geologic emissions (Table 1).

3.2. Modeling: Methane and $^{13}CH_4$ Box Model

A one-box steady state atmospheric box model based on Nicewonger et al. (2018) was used to calculate methane mixing ratios and the $\delta^{13}CH_4$ isotopic signature for a range of emission scenarios. The model includes emissions from biogenics (wetlands and agriculture), biomass and biofuel burning, and geologic outgassing. Sources were assigned a $^{13}C/^{12}C$ ratio based on the modern inventory from Schwietzke et al. (2016) with the biomass burning, biofuel burning, and biogenic sources adjusted by 1.8‰ to account for the depletion in atmospheric $\delta^{13}CO_2$ since industrialization (Rubino et al., 2013; Table S1). The model includes CH_4 losses to OH, soil, and the stratosphere and simulations are done with and without a chlorine sink. The lifetimes of CH_4 with respect to OH, soil, stratosphere, and chlorine are 11.2, 200, 120, and

Table 1
UCI-CTM Sensitivities for Ethane and Acetylene With No Cl Sink for Greenland (GRN) and Antarctica (ANT) From Different Tracer Simulations

		Fraction of total burning emissions in each region (%)		Modeled sensitivities (pmol mol^{-1}/Tg year^{-1})			
				Ethane		Acetylene	
Source	Geographic region	Ethane	Acetylene	GRN	ANT	GRN	ANT
Fossil fuel	Globe			73.9	14.2	35.3	2.8
Biofuel	Globe			79.1	16.7	37.7	3.1
Geologic	Globe			88.0	20.3	46.8	5.5
Biomass burning							
	Non-boreal (50°N to 90°S)	89.7	91.0	21.5	31.8	3.8	6.8
	Boreal (50–90°N)	10.3	9.0	214.3	4.4	106.8	0.0
	Southern Hemisphere Africa (0–35°S, 13–60°E)	24.1	25.9	12.8	33.1	0.5	6.7
	Southern Hemisphere America (0–60°S, 35–81°W)	15.8	16.9	10.1	60.7	0.5	18.9
	Australia (9–55°S, 111–168°E)	4.9	6.1	11.5	50.0	0.6	12.1
	Tropics (30°N to 30°S)	86.1	88.1	18.5	31.7	2.6	6.4
	Globe	100	100	41.4	29.0	13.1	6.2

Note. The fraction of total burning emissions from each geographic region is listed for ethane and acetylene. These values are based on the GFED3 database (van der Werf et al., 2010).

200 years, respectively (Prather et al., 2012). The isotope fractionation factors for the OH, soil, stratosphere, and chlorine sinks are 0.995, 0.980, 0.997, and 0.940, respectively (Lassey et al., 2007). The model solves the mass balance equations for CH_4, $^{12}CH_4$, and $^{13}CH_4$ and results are reported as CH_4 mole fraction (nmol mol^{-1}) and $\delta^{13}CH_4$ (per mil, ‰).

3.3. Evaluating Emission Scenarios

The UCI-CTM sensitivities were used to calculate the levels of acetylene and ethane over Greenland and Antarctica for a variety of emission scenarios by summing over the various types of emissions multiplied by the sensitivity of that emission type. In all scenarios, biofuel emissions of acetylene and ethane were fixed at 0.5 Tg year^{-1} (van Aardenne et al., 2001). The modeled Greenland and Antarctic acetylene and ethane levels were compared to the ice core observations (Table S2). Emission scenarios were evaluated for two defined time periods, the MP (1000–1500 CE) when acetylene and ethane levels were high and the Little Ice Age (LIA: 1650–1750 CE) when acetylene and ethane levels were low, using the following metrics, with acetylene as an example:

$$\Delta_{\text{acetylene, grn}} = \frac{|m_{\text{grn}} - \overline{o}_{\text{grn}}|}{\overline{o}_{\text{grn}}} \quad (2)$$

$$\Delta_{\text{acetylene, ant}} = \frac{|m_{\text{ant}} - \overline{o}_{\text{ant}}|}{\overline{o}_{\text{ant}}} \quad (3)$$

where m stands for the modeled acetylene level and $\overline{o}$ for the observed mean level of acetylene from the ice core record from Greenland (grn) and Antarctica (ant). Emissions scenarios were considered viable if $\Delta_{\text{acetylene, grn}}$ and $\Delta_{\text{acetylene, ant}}$ were both <0.1 and rejected if either $\Delta_{\text{acetylene, grn}}$ or $\Delta_{\text{acetylene, ant}}$ were >0.1 as was done in Nicewonger et al. (2018, 2020).

A similar approach was used to evaluate emission scenarios of methane calculated using the one-box model. Emissions of methane from biomass burning, microbial, and geologic sources were varied over a broad range. The resulting methane and $\delta^{13}CH_4$ from each emission scenario were compared to ice core records of CH_4 and $\delta^{13}CH_4$ (Table S2). Emission scenarios were evaluated for defined time periods by using the following metrics:

$$\Delta_{CH_4} = \frac{|m_{[CH_4]} - \overline{o}_{[CH_4]}|}{\overline{o}_{[CH_4]}} \quad (4)$$

$$\Delta_{\delta 13CH_4} = \frac{|m_{\delta 13CH_4} - \overline{o}_{\delta 13CH_4}|}{|\delta 13CH_{4_{max}} - \delta 13CH_{4_{min}}|} \quad (5)$$

Table 2
Four Emissions Scenarios Constrained by Assumptions About Geologic Emissions and Atmospheric Losses to Chlorine Atoms for Acetylene (A), Ethane (E), and Methane (M)

	Geologic emissions (Tg year^{-1})			Loss to chlorine (% of total losses)		
Scenario	A	E	M	A	E	M
noGEO-noCl	0	0	0	0	0	0
noGEO-highCl	0	0	0	0	40	5
lowGEO-noCl	0.5	2	20	0	0	0
lowGEO-highCl	0.5	2	20	0	40	5

where m and $\bar{o}$ represent modeled and observed (ice core) CH_4 and $\delta^{13}CH_4$. Emission scenarios were considered viable if Δ_{CH4} and $\Delta_{\delta 13CH4}$ were both <0.1 and rejected if either Δ_{CH4} or $\Delta_{\delta 13CH4}$ were >0.1.

3.4. Chlorine Sink

Chlorine atoms are estimated to account for roughly 1–5% of the total loss of methane (Allan et al., 2007; Prather et al., 2012; Wang et al., 2019). The reaction rate (k_{ethane}) for ethane with chlorine at 298 K is 5.69×10^{-11} cm^3 molecules^{-1} s^{-1} (Burkholder et al., 2015). The reaction rate ($k_{methane}$) for methane with chlorine at 298 K is 1.00×10^{-13} cm^3 molecules^{-1} s^{-1} (Burkholder et al., 2015). The ratio of $k_{ethane}/k_{methane}$ is roughly 569. Assuming the upper limit chlorine sink of 5% of total methane loss, the resulting methane lifetime due to chlorine loss is about 200 years (Prather et al., 2012). Using this lifetime, and the $k_{ethane}/k_{methane}$ ratio, we calculated the impact on the ethane sink as follows:

$$\frac{1}{\tau_{total}} = \frac{1}{\tau_{OH}} + \frac{1}{\tau_{Cl}} \tag{6}$$

where τ_{OH} is the lifetime of ethane due to OH oxidation (which we assumed is 2.5 months or roughly 0.21 years); τ_{Cl} is the lifetime of ethane due to chlorine oxidation, which is calculated based on the methane lifetime due to chlorine loss and the ratio of $k_{ethane}/k_{methane}$ to chlorine:

$$\tau_{Cl} = \left(\frac{200 \text{ years}}{\frac{k_{ethane}}{k_{methane}}} \right) = 0.35 \text{ years} \tag{7}$$

where 200 years is the methane lifetime due to a 5% total loss from chlorine oxidation, and $k_{ethane}/k_{methane}$ is the relative ratio between the reaction rates of ethane and methane to chlorine. The τ_{total} becomes

$$\frac{1}{\tau_{total}} = \frac{1}{0.21 \text{ year}} + \frac{1}{0.35 \text{ year}} = \frac{1}{0.13 \text{ year}} \tag{8}$$

Thus, a 5% chlorine methane sink means that about 40% of all ethane loss occurs due to reaction with chlorine. Wang et al. (2019) estimates from an oxidant-aerosol-halogen atmospheric chemistry model that chlorine contributes 1% to the global oxidation of methane and 20% to ethane. Our calculated response for ethane to chlorine oxidation is slightly less than what is expected from the Wang et al. (2019) results. Sensitivities were calculated from the UCI-CTM over a range of lifetimes for ethane, including the extreme case of a 40% chlorine sink. In doing this it was assumed that the chlorine field is identical to the OH field in the UCI-CTM, which is not necessarily correct but can be considered a reasonable approximation (Wang et al., 2019). In scenarios with chlorine oxidation enabled, the 40% case sensitivities were used for ethane (Table S3).

Table 3
Modeled Ethane Emissions for the Scenarios of Geologic Emissions and Chlorine Sink Strength

	Ethane emissions				
	MP		LIA		
Scenario	Non-boreal	Boreal	Non-boreal	Boreal	Change in total burning (%)
noGEO-noCl	3.18 ± 0.22	1.90 ± 0.14	2.09 ± 0.16	1.89 ± 0.14	−22
noGEO-highCl	5.78 ± 0.35	2.48 ± 0.18	3.95 ± 0.25	2.46 ± 0.17	−22
lowGEO-noCl	2.01 ± 0.22	1.20 ± 0.14	0.91 ± 0.15	1.19 ± 0.13	−35
lowGEO-highCl	4.57 ± 0.36	1.77 ± 0.18	2.75 ± 0.25	1.75 ± 0.17	−29

Note. All emissions are in Tg ethane per year. The reported percent changes are calculated as (MP − LIA)/MP.

Table 4
Modeled Acetylene Emissions for the Scenarios of Geologic Emissions and Chlorine Sink Strength

	Acetylene emissions				
	MP		LIA		
Scenario	Non-boreal	Boreal	Non-boreal	Boreal	Change in total burning (%)
noGEO-noCl	5.03 ± 0.30	0.62 ± 0.06	2.28 ± 0.15	0.60 ± 0.04	−49
noGEO-highCl	5.03 ± 0.30	0.62 ± 0.06	2.28 ± 0.15	0.60 ± 0.04	−49
lowGEO-noCl	4.64 ± 0.30	0.41 ± 0.06	1.89 ± 0.15	0.39 ± 0.05	−55
lowGEO-highCl	4.64 ± 0.30	0.41 ± 0.06	1.89 ± 0.15	0.39 ± 0.05	−55

Note. All emissions are in Tg acetylene per year. The reported percent changes are calculated as (MP − LIA)/MP.

4. Results and Discussion

4.1. Emissions Scenarios for the Medieval and Little Ice Age Periods

The first step in the analysis is to develop emissions scenarios for acetylene, ethane, and methane that satisfy the observed ice core data for each trace gas. In constructing those scenarios, the geologic sources of methane and ethane were limited to two possible conditions: (1) 0 or (2) the high end of the range permitted by radiocarbon measurements of ice core methane (Dyonisius et al., 2020; Hmiel et al., 2020; Petrenko et al., 2017). For acetylene, we assumed a maximum geologic emission of 0.5 Tg year^{-1} during the preindustrial based on results from Nicewonger et al. (2020), although there is no quantitative evidence to suggest the geologic acetylene source is nonzero. Similarly, two different estimates for the atmospheric chlorine sink for ethane and methane were allowed: (1) 0% for both compounds and (2) 40% and 5% for ethane and methane, respectively, based on the calculations in section 3.4. The chlorine sink is not significant for acetylene and is kept at 0% in all scenarios. These constraints result in four different emission scenarios: no geologic emissions with no chlorine sink (noGEO-noCl), no geologic emissions with a high chlorine sink (noGEO-highCl), low geologic emissions with no chlorine sink (lowGEO-noCl), and low geologic emissions with a high chlorine sink (lowGEO-highCl) (Table 2).

In the model simulations for acetylene and ethane, boreal (90–50°N) and non-boreal (90°S to 50°N) biomass burning emissions can vary independently. Greenland exhibits very high sensitivity to emissions from boreal fires, and the boreal burning emissions must be allowed to vary independently in order to simulate the different trends in Greenland and Antarctic ice cores (Nicewonger et al., 2018, 2020). In contrast, Antarctic acetylene and ethane exhibits very low sensitivity to boreal burning emissions. Antarctic ice core records of acetylene and ethane primarily reflect tropical burning, which comprises the bulk of global biomass burning emissions today based on the CTM sensitivities and geographic distribution of fires (Nicewonger et al., 2018, 2020). In the following discussion, the biomass burning acetylene and ethane emissions are reported as the sum of the emissions from boreal and non-boreal regions (see Tables 3 and 4 for breakdown). Because of the long atmospheric lifetime of methane, differences in sensitivity due to the geographic location of emissions are negligible. As such, methane emissions are also reported as global totals (Table 5).

Table 5
Modeled Methane Emissions for the Scenarios of Geologic Emissions and Cl Sink Strength

	Methane emissions					
	MP		LIA			
Scenario	Biomass burning	Microbial	Biomass burning	Microbial	Change in burning (%)	Change in microbial (%)
noGEO-noCl	32.4 ± 2.4	160.8 ± 9.2	25.6 ± 2.0	171.1 ± 9.9	−21	6
noGEO-highCl	21.6 ± 1.8	180.8 ± 10.1	14.3 ± 1.6	192.4 ± 11.5	−34	6
lowGEO-noCl	23.6 ± 2.4	149.5 ± 9.2	16.8 ± 2.0	159.8 ± 9.9	−29	7
lowGEO-highCl	13.1 ± 1.9	170.8 ± 10.3	5.6 ± 1.4	181.5 ± 11.0	−57	6

Note. All emissions are in Tg methane per year. The reported percent changes are calculated as (MP − LIA)/MP.

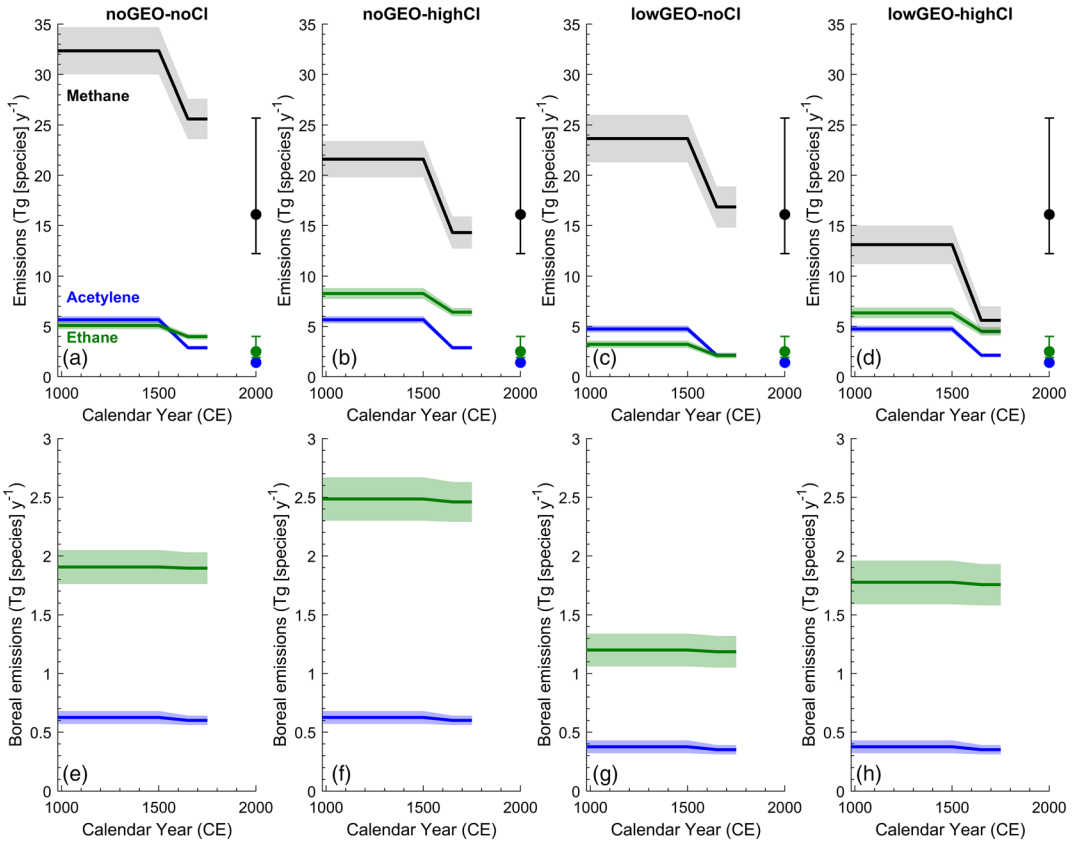

Figure 3. (a–h) Biomass burning scenarios for acetylene (blue), ethane (green), and methane (black) for various estimates of the geologic source and Cl sink. Boreal emissions for acetylene and ethane are separated in the bottom panels (e–h). Shaded regions reflect uncertainties in the emissions and the emission factors. Modern emission estimates based on GFED4 and emission factors are shown with the colored circles.

There are similarities in the inferred biomass burning emissions of acetylene, ethane, and methane over the last 1,000 years in the four emission scenarios (Figure 3). There is a large decline in biomass burning emissions for all three gases from the MP (1000–1500 CE) to the LIA (1650–1750 CE). The acetylene history exhibits a 49–55% decline from the MP to the LIA with most of this due to a reduction in non-boreal (tropical) emissions. For methane and ethane, the decline in emissions from the MP to LIA are 21–57% and 22–35%, respectively. The ranges reflect the different constraints imposed by the geologic source strength and atmospheric chlorine sink (Figure 3).

4.2. Is there a Single Preindustrial Fire History Consistent With Acetylene, Ethane, and Methane Ice Core Records?

Emissions of acetylene, ethane, and methane from biomass burning are not equal by mass (i.e., not 1-g acetylene to 1-g methane), and so comparing the inferred biomass burning histories of these compounds together cannot allow us to answer the question of whether the ice core gas records indicate a single fire history. A fire history (dry matter burned) can be derived from each of the trace gas emission histories as follows:

$$H\left(\frac{\text{kg dry matter}}{y}\right) = \frac{E\left(\frac{\text{g trace gas}}{y}\right)}{EF\left(\frac{\text{g trace gas}}{\text{kg dry matter}}\right)} \tag{9}$$

where H is the fire history, E is the emissions history based on the ice core data, and EF is the trace gas specific emission factor. For this calculation we used boreal and non-boreal biome-weighted emission factors for acetylene and ethane, and a globally weighted emission factor for methane, assuming the same

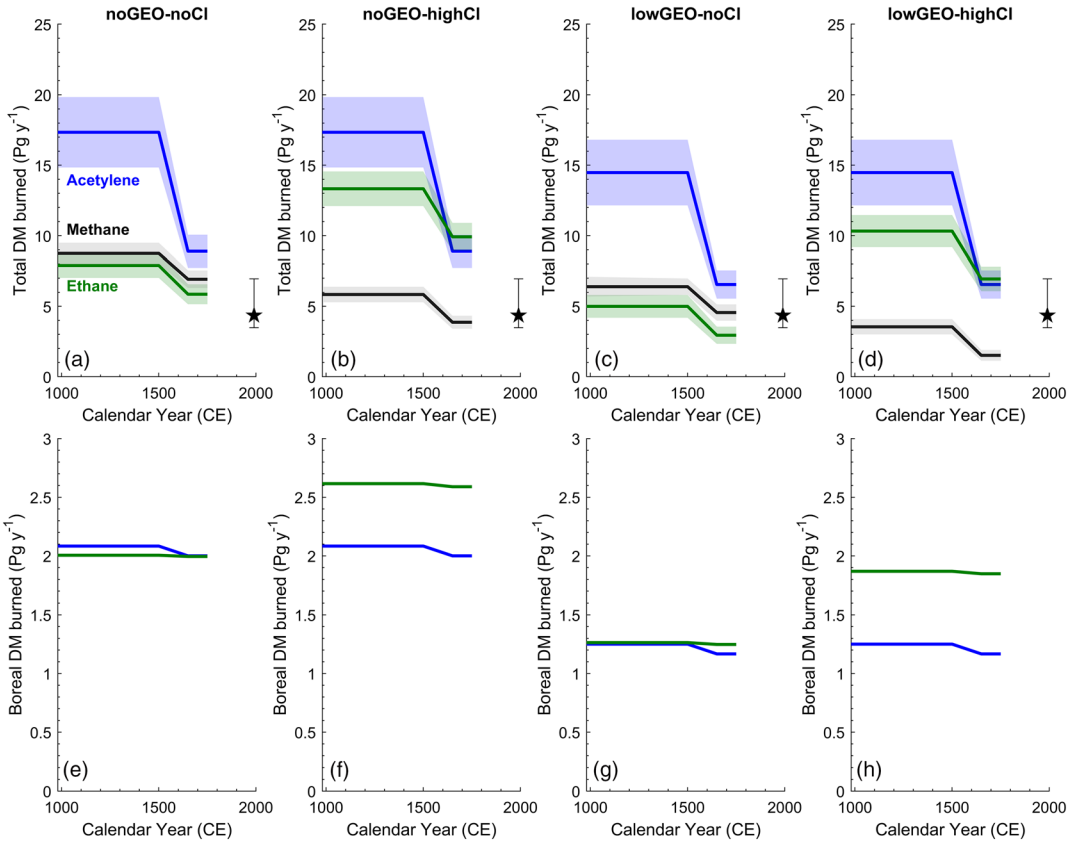

Figure 4. Dry matter burned inferred from each gas record (a–d) and the resulting boreal dry matter burned (e–h). Shaded regions reflect the 1σ uncertainties in emissions and emission factors, which propagate into the calculation of dry matter. Modern estimate of dry matter burned from GFED4 is shown with the black star.

geographic footprint and distribution of biomes as the GFED4 inventory (Tables S5 and S6). In accordance with the trace gas histories, the fire histories show a large decline from the MP to the LIA, and the results exhibit sensitivity to assumptions about the chlorine sink and geologic emissions (Figure 4 and Table 6).

The fire histories (dry matter burned) inferred from the three gases for the past 1,000 years do not agree under the admittedly unrealistic assumption of modern fire and biogeography. At most two of the trace gases yield similar dry matter burned histories for any of the four model scenarios. Interestingly, the shortest-lived gas, acetylene, yields the highest dry matter burned through time in all scenarios. This suggests that changes in the geographic distribution of fires could reconcile the burning histories. For example, sedimentary charcoal records in various locations across the globe depict different fire activity histories (e.g., Marlon et al., 2008 ; Power et al., 2012). South American speleothem proxy records suggest a southward shift in the location of the Intertropical Convergence Zone (ITCZ) during the Little Ice Age leading to an enhanced South American summer monsoon (Haug et al., 2001; Sachs et al., 2009; Vuille et al., 2012). One could

Table 6
Dry Matter Burned (Pg year^{-1}) Inferred From the Three Ice Core Gas Records

	Acetylene			*Ethane*			*Methane*		
Scenario	MP	LIA	% decline	MP	LIA	% decline	MP	LIA	% decline
noGEO-noCl	17.34 ± 2.50	8.89 ± 1.17	49	7.89 ± 0.88	5.86 ± 0.71	26	8.74 ± 0.75	6.91 ± 0.62	21
noGEO-highCl	17.34 ± 2.50	8.89 ± 1.17	49	13.33 ± 1.23	9.91 ± 0.99	26	5.84 ± 0.55	3.86 ± 0.46	34
lowGEO-noCl	14.48 ± 2.33	6.55 ± 1.00	55	4.99 ± 0.81	2.94 ± 0.61	41	6.39 ± 0.75	4.55 ± 0.62	28
lowGEO-highCl	14.48 ± 2.33	6.55 ± 1.00	55	10.32 ± 1.14	6.94 ± 0.87	33	3.54 ± 0.54	1.51 ± 0.38	57

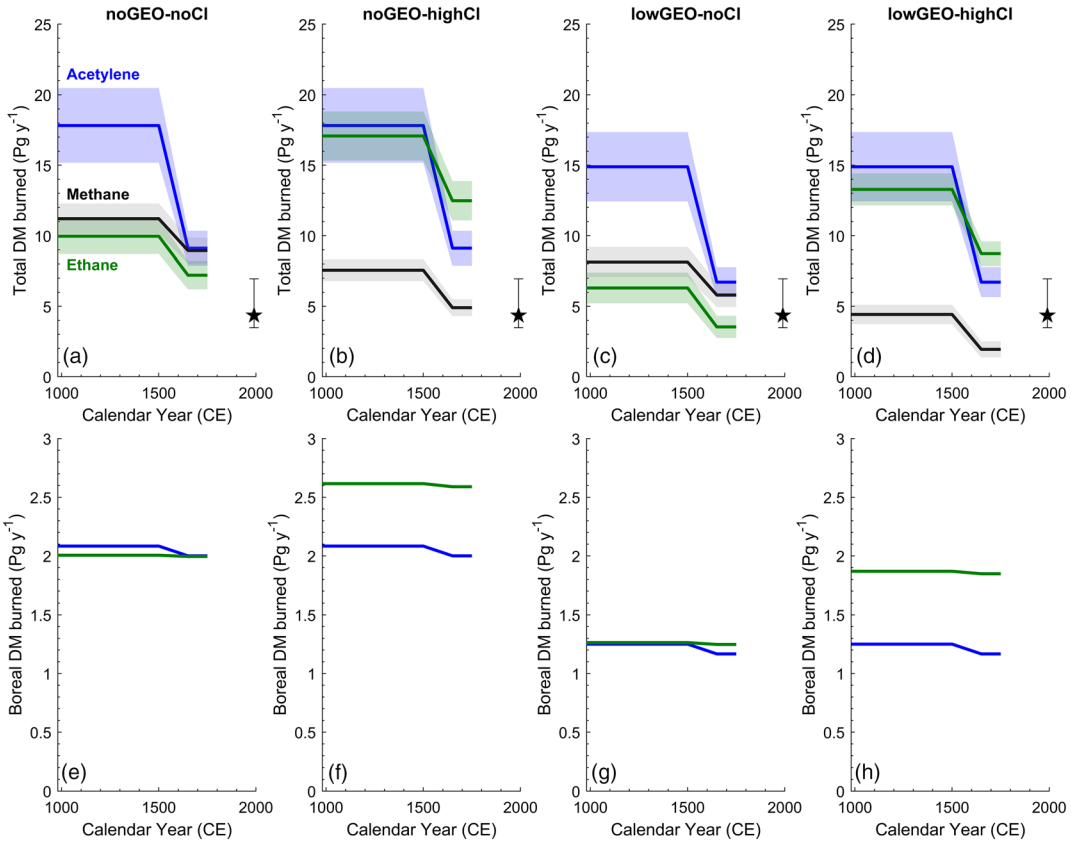

Figure 5. Dry matter burned inferred from each gas record assuming all non-boreal biomass burning emission resulted from savanna/grasslands burning (all-SAV; top row). Shaded regions and stars are same as in Figure 4.

hypothesize that shifting the ITCZ north or south impacts the location and extent of tropical burning which could result in the observations in the charcoal records (Marlon et al., 2008; Power et al., 2012). Such shifts could also influence the transport of the shorter-lived gases (acetylene and ethane) to the polar regions. Human activities also likely influenced the spatial distribution of burning. Pollen records in Meso- and South America during the last 2,000 years show a succession from forests to savanna, likely driven by human activities (Flantua et al., 2016). Pollen studies in New Zealand also show shifts in vegetation due to human activities (Elliot et al., 1998). Additional changes to the vegetation landscape occurred after the catastrophic depopulation that occurred in the Americas following European contact in the mid to late fourteenth century (Koch et al., 2019).

4.2.1. Sensitivity to Changes in the Spatial Distribution of Biomes and Biomass Burning

Since a single fire history was unable to be reconstructed simply by scaling the modern distribution of fire, three additional model scenarios were constructed to explore the sensitivity of fire histories to possible changes in the spatial distributions of biomes and burning. Relative changes in regional burning patterns have been inferred from the global charcoal database and changes in biomes have been inferred from pollen and land use records (Marlon et al., 2008; Pongratz et al., 2008; Power et al., 2012). Rather than try to reproduce specific patterns of change implied by these records, we focused on a few extreme cases to test the limits of whether such changes could reconcile the burning histories from the three trace gases. These scenarios are described below.

1. All savanna/grassland (*all-SAV*) — This scenario is designed to examine the possibility that trace gas emission factors were different in the past due to variations in the spatial patterns of the types of vegetation (Pongratz et al., 2008). As an extreme case, we assumed that all the paleobiomass from the non-boreal zone had the trace gas emission factor of savanna/grassland (which comprises about 67% of dry matter burned today). These factors are lower than the GFED4 global weighted mean emission factor, which

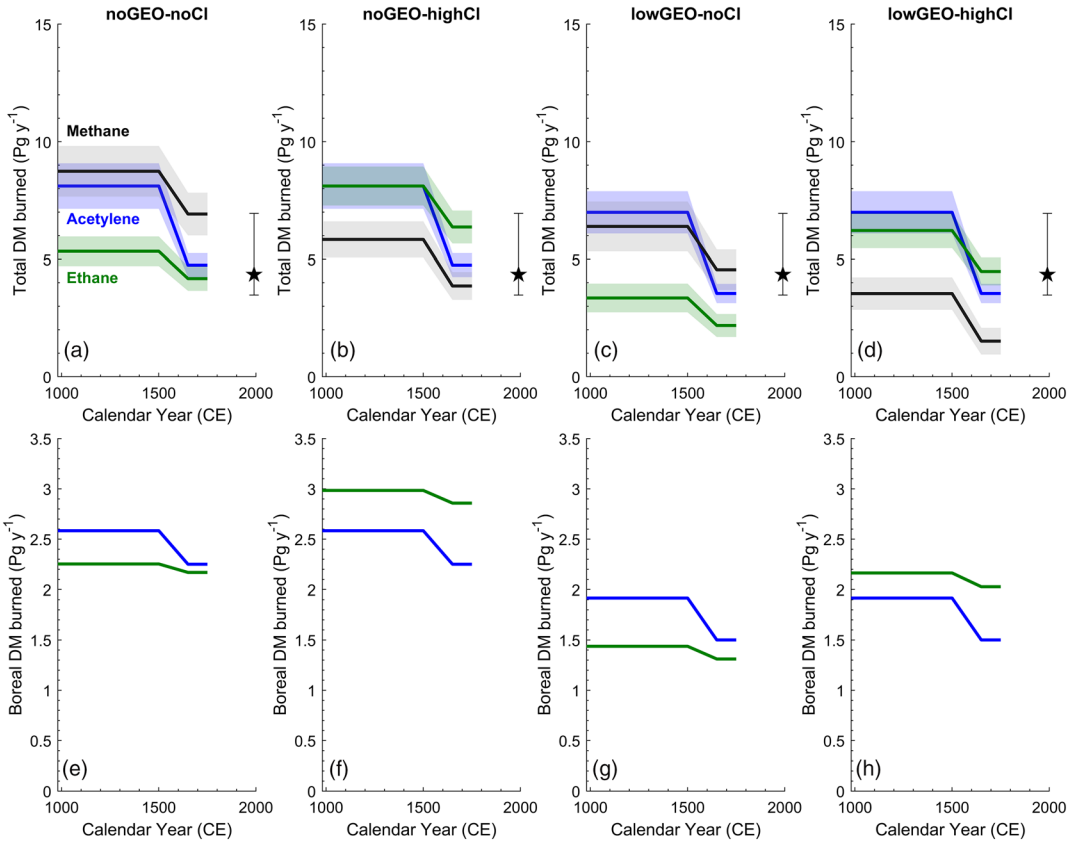

Figure 6. Dry matter burned inferred from each gas record assuming all biomass burning emissions were in the South America region (all-SA). Shaded regions and stars are same as in Figure 4. Note the vertical axes in the top row now range from 0–15 Pg year^{-1}.

considers all biomes in the non-boreal zone weighted by their total contribution to non-boreal emissions, so a correspondingly larger dry matter burned is required to achieve the same biomass burning emissions of each gas. In addition, the $^{13}CH_4$ source end-member for biomass burning was changed to −12‰ to represent an all grassland dominated fire-regime (Farquhar et al., 1989; Ferretti et al., 2005). The *all-SAV* fire characteristics were applied to all four of the scenarios in Table 2. The results show only a slight reduction in the discrepancies between the inferred dry matter burned from acetylene, ethane, and methane (Figure 5). Clearly, changing the emission factors to result in the highest ratio of emission to dry matter burned alone cannot resolve these discrepancies between the inferred dry matter histories from the three gases.

2. All South America (*all-SA*) — It is possible that the discrepancies observed in the dry matter burned using the modern spatial distribution of fires may be due to the fact that the location of fires has changed over the past 1,000 years. The abundances of shorter-lived trace gases in the atmosphere over the polar regions are sensitive to the location of fire emissions. Acetylene and ethane over Antarctica exhibit the highest sensitivity to emissions from South America as compared to any other southern latitude site (Table 1). To test the influence of spatial changes in the distribution of fire, we moved all non-boreal biomass burning ethane and acetylene emissions to South America (Figure 6), while keeping the same vegetation type distribution in South America as modern day (i.e., no changes to the emission factors). This reduces the burning required for these compounds relative to that for the longer-lived methane, which is insensitive to the location of emissions. The required dry matter burned from acetylene and ethane is significantly reduced and there is better agreement between the inferred dry matter burned histories from all the gases. It is important to emphasize that this is an extreme, and climatically unrealistic case, but it tests the upper limits of the hypothesis that the location of fires in the preindustrial was different than the modern era. Even in this improbable case, there is no scenario in which all three inferred dry

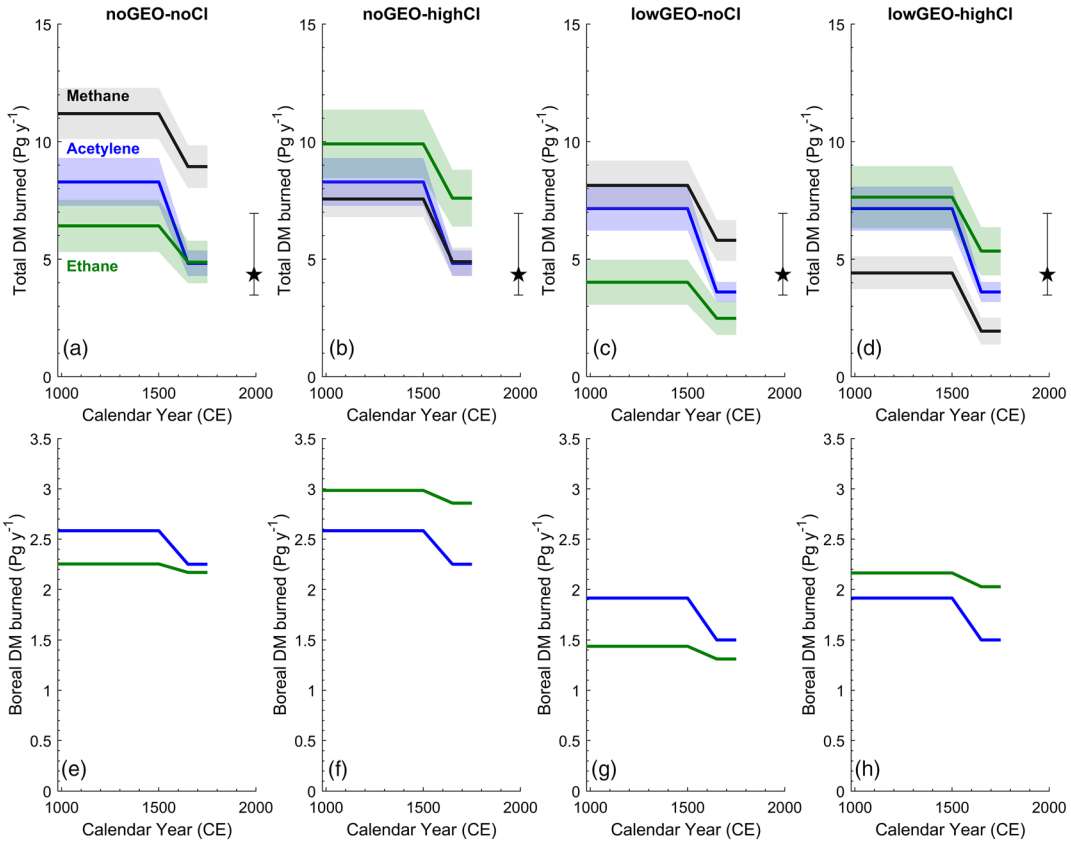

Figure 7. Dry matter burned inferred from each gas record assuming all biomass burning emissions were in the South America region and were from the savanna/grassland biome. Shaded regions and stars are same as in Figure 4. Note the vertical axes in the top row ranges from 0–15 Pg year^{-1}.

matter burned histories agree within their analytical uncertainties. This suggests that changes to the location of fires in the past cannot solely explain the differences observed in the dry matter histories from acetylene, ethane, and methane.

3. All savanna/grassland and all South America (*all-SAV-SA*) — Here the two previous cases are combined, with savanna/grassland emission ratios and all burning in South America. In this case, there is only one scenario in which all three inferred dry matter burned histories agree within estimated uncertainties (Figure 7). This is the case where ethane and methane have no geologic emissions and a high chlorine sink.

4.2.2. Sensitivity to Assumptions About Biofuel Emissions

The modern-day distribution of biofuel emissions used in our calculations may not reflect the preindustrial conditions (Yevich & Logan, 2003). Koch et al. (2019) suggest that MP indigenous populations, located in the Caribbean, Mexico, Central America, Inca Territory, Amazonia, South America, and North America, were roughly 60.5 million. Most of this population was in the tropics (30°S to 30°N). There is strong consensus that these populations relied heavily on biofuels. If biofuel emissions in the preindustrial were greater than previously thought and were more concentrated in the tropics than the modern inventory suggests, the required biomass burning emission scenarios implied from this work would be lower. However, replacing non-boreal (tropical) biomass burning emissions with tropically located biofuel emissions would be a roughly 1:1 trade off and would require the same total emissions to reconstruct the acetylene and ethane records. Reconstructing a single fire history from acetylene, ethane, and methane would still be challenging unless the biofuel sources (1) were heavily distributed toward the higher southern latitudes (>30°S) and (2) were heavily enriched in acetylene emissions over ethane and methane emissions. Emission factors from multiple biomass types do not indicate that this is realistic (Akagi et al., 2011; Andreae, 2019; Andreae & Merlet, 2001).

4.2.3. Sensitivity to Changes in Methane Source Isotopic End-Members

The biomass burning histories of methane reconstructed here are sensitive to the isotopic end-members assigned to each source. It is likely that the methane isotope end-members are dynamic and change through time, particularly due to ecosystem shifts and changes in climate (Sowers, 2010). The complicated nature of the methane isotope budget makes interpreting paleobiomass burning emissions challenging, particularly over long time periods, and during periods of large climate shifts. We are unable to fully address all the complexities of the methane budget in this study, but acknowledge that some of the differences in the fire histories between acetylene, ethane, and methane may be due to the methane isotopic-end-member values used in our model.

5. Conclusions

The focus of this study is on developing a quantitative record of changes in biomass burning over the past millennium. Ice core gas records are among the only truly quantitative methods of inferring burning because the atmosphere physically integrates emissions across the planet. In this study, we show that ice core records of acetylene, ethane, and methane do not readily yield a single fire history even allowing dramatic changes in the distribution of fires and vegetation types. Uncertainties in background geologic emissions of ethane and methane and the chorine sink likely do not account for the differences in the dry matter burned histories derived from the three trace gases. One could argue that the results for methane are most uncertain, given the complexity of the budget, the difficulty in establishing whether isotopic end-members remain constant in time, and assumptions about changes in microbial emissions. Putting aside methane, the best agreement in the acetylene and ethane dry matter burned histories is from scenarios in which ethane has a large chlorine sink, consistent with recent modeling work by Wang et al. (2019). This suggests that chlorine plays an important role in the global ethane budget and should be included in future analyses. The history of atmospheric hydrocarbons in polar ice clearly contains a wealth of useful information about the history of burning. However, further work is needed to fully understand those records in a quantitative sense.

Data Availability Statement

Acetylene and ethane ice core data are available online (https://doi.org/10.18739/A2J09W45H). The methane box model code and the ethane and acetylene emission search code are available online (at https://doi.org/10.7280/D14X2M).

Acknowledgments
We thank Xin Zhu for assistance with the UCI-CTM, and NSF-ICF and IDP for the ice core drilling and sampling assistance.

References

Akagi, S. K., Yokelson, R. J., Wiedinmyer, C., Alvarado, M. J., Reid, J. S., Karl, T., et al. (2011). Emission factors for open and domestic biomass burning for use in atmospheric models. *Atmospheric Chemistry and Physics*, *11*(9), 4039–4072. https://doi.org/10.5194/acp-11-4039-2011

Allan, W., Struthers, H., & Lowe, D. C. (2007). Methane carbon isotope effects caused by atomic chlorine in the marine boundary layer: Global model results compared with Southern Hemisphere measurements. *Journal of Geophysical Research*, *112*, D04306. https://doi.org/10.1029/2006JD007369

Andela, N., Morton, D. C., Giglio, L., Chen, Y., van der Werf, G. R., Kasibhatla, P. S., et al. (2017). A human-driven decline in global burned area. *Science*, *356*, 1356–1362. https://doi.org/10.1126/science.aal4108

Anderson, R. C. (1958). Acetylene as an intermediate in combustion of petroleum hydrocarbons. *Advances in Chemistry*, *20*, 49–57. https://doi.org/10.1021/ba-1958-0020.ch005

Andreae, M. O. (2019). Emission of trace gases and aerosols from biomass burning—An updated assessment. *Atmospheric Chemistry and Physics*, *19*, 8523–8546. https://doi.org/10.5194/acp-19-8523-2019

Andreae, M. O., & Merlet, P. (2001). Emission of trace gases and aerosols from biomass burning. *Global Biogeochemical Cycles*, *15*, 955–966. https://doi.org/10.1029/2000GB001382

Archibald, S., Roy, D. P., van Wilgen, B. W., & Scholes, R. J. (2009). What limits fire? An examination of drivers of burnt area in Southern Africa. *Global Change Biology*, *15*, 613–630. https://doi.org/10.1111/j.1365-2486.2008.01754.x

Aydin, M., Verhulst, K. R., Saltzman, E. S., Battle, M. O., Montzka, S. A., Blake, D. R., et al. (2011). Recent decreases in fossil-fuel emissions of ethane and methane derived from firn air. *Nature*, *476*, 198–201. https://doi.org/10.1038/nature10352

Beck, J., Bock, M., Schmitt, J., Seth, B., Blunier, T., & Fischer, H. (2018). Bipolar carbon and hydrogen isotope constraints on the Holocene methane budget. *Biogeosciences*, *15*, 7155–7175. https://doi.org/10.5194/bg-15-7155-2018

Bock, M., Schmitt, J., Beck, J., Seth, B., Chappellaz, J., & Fischer, H. (2017). Glacial/interglacial wetland, biomass burning, and geologic methane emissions constrained by dual stable isotopic CH_4 ice core records. *Proceedings of the National Academy of Sciences*, *114*, E5778–E5786. https://doi.org/10.1073/pnas.1613883114

Bowman, D. M. J. S., Balch, J., Artaxo, P., Bond, W. J., Cochrane, M. A., D'Antonio, C. M., et al. (2011). The human dimension of fire regimes on Earth. *Journal of Biogeography*, *38*, 2223–2236. https://doi.org/10.1111/j.1365-2699.2011.02595.x

Bowman, D. M. J. S., Balch, J. K., Artaxo, P., Bond, W. J., Carlson, J. M., Cochrane, M. A., et al. (2009). Fire in the Earth system. *Science*, *324*, 481–484. https://doi.org/10.1126/science.1163886

Burkholder, J. B., Sander, S. P., Abbatt, J., Barker, J. R., Huie, R. E., Kolb, C. E., et al. (2015). *Chemical kinetics and photochemical data for use in atmospheric studies evaluation no. 18*. Pasadena: JPL publication 15-10, jet Propulsion Laboratory. https://jpldataeval.jpl.nasa.gov

Clarkson, T. S., Martin, R. J., & Rudolph, J. (1997). Ethane and propane in the southern marine troposphere. *Atmospheric Environment*, *31*, 3763–3771. https://doi.org/10.1016/S1352-2310(97)00220-3

Dalsøren, S. B., Myhre, G., Hodnebrog, Ø., Myhre, C. L., Stohl, A., Pisso, I., et al. (2018). Discrepancy between simulated and observed ethane and propane levels explained by underestimated fossil emissions. *Nature Geoscience*, *11*, 178–184. https://doi.org/10.1038/s41561-018-0073-0

Dlugokencky, E. J., Nisbet, E. G., Fisher, R., & Lowry, D. (2011). Global atmospheric methane: Budget, changes and dangers. *Philosophical Transactions of the Royal Society A: Mathematical, Physical and Engineering Sciences*, *369*, 2058–2072. https://doi.org/10.1098/rsta.2010.0341

Dyonisius, M. N., Petrenko, V. V., Smith, A. M., Hua, Q., Yang, B., Schmitt, J., et al. (2020). Old carbon reservoirs were not important in the deglacial methane budget. *Science*, *367*, 907–910. https://doi.org/10.1126/science.aax0504

Elliot, M. B., Flenley, J. R., & Sutton, D. G. (1998). A late Holocene pollen record of deforestation and environmental change from the Lake Tauanui catchment, Northland, New Zealand. *Journal of Paleolimnology*, *19*, 23–32. https://doi.org/10.1023/A:100792102

Etheridge, D. M., Steele, L. P., Francey, R. J., & Langenfelds, R. L. (1998). Atmospheric methane between 1000 A.D. and present: Evidence of anthropogenic emissions and climatic variability. *Journal of Geophysical Research*, *103*, 15,979–15,993. https://doi.org/10.1029/98JD00923

Etiope, G. (2012). Climate science: Methane uncovered. *Nature Geoscience*, *5*, 373–374. https://doi.org/10.1038/ngeo1483

Etiope, G., & Ciccioli, P. (2009). Earth's degassing: A missing ethane and propane source. *Science*, *323*, 478. https://doi.org/10.1126/science.1165904

Etiope, G., & Schwietzke, S. (2019). Global geological methane emissions: An update of top-down and bottom-up estimates. *Elementa: Science of the Anthropocene*, *7*, 1–9. https://doi.org/10.1525/elementa.383

Farquhar, G. D., Ehleringer, J. R., & Hubick, K. T. (1989). Carbon isotope discrimination and photosynthesis. *Annual Review of Plant Physiology and Plant Molecular Biology*, *40*, 503–537. https://doi.org/10.1146/annurev.pp.40.060189.002443

Ferretti, D. F., Miller, J. B., White, J. W. C., Etheridge, D. M., Lassey, K. R., Lowe, D. C., et al. (2005). Unexpected changes to the global methane budget over the past 2000 years. *Science*, *309*, 1714–1717. https://doi.org/10.1126/science.1115193

Flantua, S. G. A., Hooghiemstra, H., Vuille, M., Behling, H., Carson, J. F., Gosling, W. D., et al. (2016). Climate variability and human impact in South America during the last 2000 years: Synthesis and perspectives from pollen records. *Climate of the Past*, *12*, 483–523. https://doi.org/10.5194/cp-12-483-2016

Franco, B., Mahieu, E., Emmons, L. K., Tzompa-Sosa, Z. A., Fischer, E. V., Sudo, K., et al. (2016). Evaluating ethane and methane emissions associated with the development of oil and natural gas extraction in North America. *Environmental Research Letters*, *11*, 044010. https://doi.org/10.1088/1748-9326/11/4/044010

Giglio, L., Randerson, J. T., & van der Werf, G. R. (2013). Analysis of daily, monthly, and annual burned area using the fourth-generation global fire emissions database (GFED4). *Journal of Geophysical Research: Biogeosciences*, *118*, 317–328. https://doi.org/10.1002/jgrg.20042

Grieman, M. M., Aydin, M., Fritzsche, D., McConnell, J. R., Opel, T., Sigl, M., & Saltzman, E. S. (2017). Aromatic acids in a Eurasian Arctic ice core: A 2600-year proxy record of biomass burning. *Climate of the Past*, *13*(4), 395–410. https://doi.org/10.5194/cp-13-395-2017

Grieman, M. M., Aydin, M., Isaksson, E., Schwikowski, M., & Saltzman, E. S. (2018). Aromatic acids in an Arctic ice core from Svalbard: A proxy record of biomass burning. *Climate of the Past*, *14*(5), 637–651. https://doi.org/10.5194/cp-14-637-2018

Grieman, M. M., Aydin, M., McConnell, J. R., & Saltzman, E. S. (2018). Burning-derived vanillic acid in an Arctic ice core from Tunu, northeastern Greenland. *Climate of the Past*, *14*(11), 1625–1637. https://doi.org/10.5194/cp-14-1625-2018

Gunter, B. D., & Musgrave, B. C. (1971). New evidence on the origin of methane in hydrothermal gases. *Geochimica et Cosmochimica Acta*, *35*, 113–118. https://doi.org/10.1016/0016-7037(71)90109-8

Hantson, S., Arneth, A., Harrison, S. P., Kelley, D. I., Prentice, I. C., Rabin, S. S., et al. (2016). The status and challenge of global fire modelling. *Biogeosciences*, *13*, 3359–3375. https://doi.org/10.5194/bg-13-3359-2016

Haug, G. H., Hughen, K. A., Sigman, D. M., Peterson, L. C., & Ro, U. (2001). Southward migration of the Intertropical Convergence Zone through the Holocene. *Science*, *293*, 1304–1308. https://doi.org/10.1126/science.1059725

Helmig, D. (2017). Atmospheric hydrocarbons as tracers for climate change, air transport, and oxidation chemistry in the Arctic, GEOSummit, Greenland 2008–2017. Arctic Data Center. https://doi.org/10.18739/A2RS0X

Helmig, D., Rossabi, S., Hueber, J., Tans, P., Montzka, S. A., Masarie, K., et al. (2016). Reversal of global atmospheric ethane and propane trends largely due to US oil and natural gas production. *Nature Geoscience*, *9*, 490–495. https://doi.org/10.1038/ngeo2721

Hmiel, B., Petrenko, V. V., Dyonisius, M. N., Buizert, C., Smith, A. M., Place, P. F., et al. (2020). Preindustrial $^{14}CH_4$ indicates greater anthropogenic fossil CH4 emissions. *Nature*, *578*, 409–412. https://doi.org/10.1038/s41586-020-1991-8

Holmes, C. D., Prather, M. J., Sovde, O. A., & Myhre, G. (2013). Future methane, hydroxyl, and their uncertainties: Key climate and emission parameters for future predictions. *Atmospheric Chemistry and Physics*, *13*, 285–302. https://doi.org/10.5194/acp-13-285-2013

Kawamura, K., Izawa, Y., Mochida, M., & Shiraiwa, T. (2012). Ice core records of biomass burning tracers (levoglucosan and dehydroabietic, vanillic and p-hydroxybenzoic acids) and total organic carbon for past 300years in the Kamchatka Peninsula, Northeast Asia. *Geochimica et Cosmochimica Acta*, *99*, 317–329. https://doi.org/10.1016/j.gca.2012.08.006

Kehrwald, N., Zangrando, R., Gabrielli, P., Jaffrezo, J., Boutron, C., Barbante, C., & Gambaro, A. (2012). Levoglucosan as a specific marker of fire events in Greenland snow. *Tellus B: Chemical and Physical Meteorology*, *64*, 1. https://doi.org/10.3402/tellusb.v64i0.18196

Kirschke, S., Bousquet, P., Ciais, P., Saunois, M., Canadell, J. G., Dlugokencky, E. J., et al. (2013). Three decades of global methane sources and sinks. *Nature Geoscience*, *6*, 813–823. https://doi.org/10.1038/ngeo1955

Knipping, E. M., & Dabdub, D. (2003). Impact of chlorine emissions from sea-salt aerosol on coastal urban ozone. *Environmental Science and Technology*, *37*, 275–284. https://doi.org/10.1021/es025793z

Koch, A., Brierley, C., Maslin, M. M., & Lewis, S. L. (2019). Earth system impacts of the European arrival and Great Dying in the Americas after 1492. *Quaternary Science Reviews*, *207*, 13–36. https://doi.org/10.1016/j.quascirev.2018.12.004

Lamarque, J. F., Bond, T. C., Eyring, V., Granier, C., Heil, A., Klimont, Z., et al. (2010). Historical (1850–2000) gridded anthropogenic and biomass burning emissions of reactive gases and aerosols: Methodology and application. *Atmospheric Chemistry and Physics*, *10*, 7017–7039. https://doi.org/10.5194/acp-10-7017-2010

Lassey, K. R., Etheridge, D. M., Lowe, D. C., Smith, A. M., & Ferretti, D. F. (2007). Centennial evolution of the atmospheric methane budget: What do the carbon isotopes tell us? *Atmospheric Chemistry and Physics*, *7*, 2119–2139. https://doi.org/10.5194/acp-7-2119-2007

Lawler, M. J., Finley, B. D., Keene, W. C., Pszenny, A. A. P., Read, K. A., von Glasow, R., & Saltzman, E. S. (2009). Pollution-enhanced reactive chlorine chemistry in the eastern tropical Atlantic boundary layer. *Geophysical Research Letters*, *36*, L08810. https://doi.org/10.1029/2008GL036666

Legrand, M., De Angelis, M., Staffelbach, T., Neftel, A., & Stauffer, B. (1992). Large perturbations of ammonium and organic acids content in the summit-Greenland Ice Core. Fingerprint from forest fires? *Geophysical Research Letters*, *19*(5), 473–475. https://doi.org/10.1029/91GL03121

Legrand, M., McConnell, J., Fischer, H., Wolff, E. W., Preunkert, S., Arienzo, M., et al. (2016). Boreal fire records in Northern Hemisphere ice cores: A review. *Climate of the Past*, *12*, 2033–2059. https://doi.org/10.5194/cp-12-2033-2016

Liu, Y., Zhang, Q., & Wang, T. (2017). Detailed chemistry modeling of partial combustion of natural gas for coproducing acetylene and syngas. *Combustion Science and Technology*, *189*, 908–922. https://doi.org/10.1080/00102202.2016.1256879

MacFarling Meure, C., Etheridge, D., Trudinger, C., Steele, P., Langenfelds, R., van Ommen, T., et al. (2006). Law dome CO_2, CH_4 and N_2O ice core records extended to 2000 years BP. *Geophysical Research Letters*, *33*, L14810. https://doi.org/10.1029/2006GL026152

McConnell, J. R., Edwards, R., Kok, G. L., Flanner, M. G., Zender, C. S., Saltzman, E. S., et al. (2007). 20th-Century Industrial Black Carbon Emissions Altered Arctic Climate Forcing. *Science*, *317*(5843), 1381–1384. https://doi.org/10.1126/science.1144856

Marlon, J. R., Bartlein, P. J., Carcaillet, C., Gavin, D. G., Harrison, S. P., Higuera, P. E., et al. (2008). Climate and human influences on global biomass burning over the past two millennia. *Nature Geoscience*, *2*, 307–702. https://doi.org/10.1038/ngeo468

Marlon, J. R., Bartlein, P. J., Daniau, A.-L., Harrison, S. P., Maezumi, S. Y., Power, M. J., et al. (2013). Global biomass burning: A synthesis and review of Holocene paleofire records and their controls. *Quaternary Science Reviews*, *65*, 5–25. https://doi.org/10.1016/j.quascirev.2012.11.029

Marlon, J. R., Kelly, R., Daniau, A., Vannière, B., Power, M. J., Bartlein, P., et al. (2016). Reconstructions of biomass burning from sediment-charcoal records to improve data—Model comparisons. *Biogeosciences*, *13*, 3225–3244. https://doi.org/10.5194/bg-13-3225-2016

Mischler, J. A., Sowers, T. A., Alley, R. B., Battle, M., McConnell, J. R., Mitchell, L., et al. (2009). Carbon and hydrogen isotopic composition of methane over the last 1000 years. *Global Biogeochemical Cycles*, *23*, GB4024. https://doi.org/10.1029/2009GB003460

Mitchell, L. E., Brook, E. J., Sowers, T., McConnell, J. R., & Taylor, K. (2011). Multidecadal variability of atmospheric methane, 1000–1800 C.E. *Journal of Geophysical Research*, *116*, G02007. https://doi.org/10.1029/2010JG001441

Nicewonger, M. R., Aydin, M., Prather, M. J., & Saltzman, E. S. (2018). Large changes in biomass burning over the last millennium inferred from paleoatmospheric ethane in polar ice cores. *Proceedings of the National Academy of Sciences*, *115*, 12,413–12,418. https://doi.org/10.1073/pnas.1807172115

Nicewonger, M. R., Aydin, M., Prather, M. J., & Saltzman, E. S. (2020). Reconstruction of paleofire emissions over the past millennium from measurements of ice core acetylene. *Geophysical Research Letters*, *47*, e2019GL085101. https://doi.org/10.1029/2019GL085101

Nicewonger, M. R., Verhulst, K. R., Aydin, M., & Saltzman, E. S. (2016). Preindustrial atmospheric ethane levels inferred from polar ice cores: A constraint on the geologic sources of atmospheric ethane and methane. *Geophysical Research Letters*, *43*, 214–221. https://doi.org/10.1002/2015GL066854

Nisbet, E. G., Dlugokencky, E. J., & Bousquet, P. (2014). Methane on the rise—Again. *Science*, *343*, 493–495. https://doi.org/10.1126/science.1247828

Petrenko, V. V., Smith, A. M., Schaefer, H., Riedel, K., Brook, E., Baggenstos, D., et al. (2017). Minimal geological methane emissions during the Younger Dryas–Preboreal abrupt warming event. *Nature*, *548*, 443–446. https://doi.org/10.1038/nature23316

Plass-Dülmer, C., Koppmann, R., Ratte, M., & Rudolph, J. (1995). Light nonmethane hydrocarbons in seawater. *Global Biogeochemical Cycles*, *9*, 79–100. https://doi.org/10.1029/94GB02416

Poisson, N., Kanakidou, M., & Crutzen, P. J. (2000). Impact of non-methane hydrocarbons on tropospheric chemistry and the oxidizing power of the global troposphere: 3-dimensional modelling results. *Journal of Atmospheric Chemistry*, *36*, 157–230. https://doi.org/10.1023/A:1006300616544

Pongratz, J., Reick, C., Raddatz, T., & Claussen, M. (2008). A reconstruction of global agricultural areas and land cover for the last millennium. *Global Biogeochemical Cycles*, *22*, GB3018. https://doi.org/10.1029/2007GB003153

Power, M. J., Marlon, J., Ortiz, N., Bartlein, P. J., Harrison, S. P., Mayle, F. E., et al. (2008). Changes in fire regimes since the last glacial maximum: An assessment based on a global synthesis and analysis of charcoal data. *Climate Dynamics*, *30*, 887–907. https://doi.org/10.1007/s00382-007-0334-x

Power, M. J., Mayle, F. E., Bartlein, P. J., Marlon, J. R., Anderson, R. S., Behling, H., et al. (2012). Climatic control of the biomass-burning decline in the Americas after AD 1500. *The Holocene*, *23*, 3–13. https://doi.org/10.1177/0959683612450196

Pozzer, A., Pollmann, J., Taraborrelli, D., Jöckel, P., Helmig, D., Tans, P., et al. (2010). Observed and simulated global distribution and budget of atmospheric C2-C5 alkanes. *Atmospheric Chemistry and Physics*, *10*, 4403–4422. https://doi.org/10.5194/acp-10-4403-2010

Prather, M. J. (1994). Lifetimes and eigenstates in atmospheric chemistry. *Geophysical Research Letters*, *21*, 801–804. https://doi.org/10.1029/94GL00840

Prather, M. J., Holmes, C. D., & Hsu, J. (2012). Reactive greenhouse gas scenarios: Systematic exploration of uncertainties and the role of atmospheric chemistry. *Geophysical Research Letters*, *39*, L09803. https://doi.org/10.1029/2012GL051440

Prather, M. J., & Hsu, J. (2010). Coupling of nitrous oxide and methane by global atmospheric chemistry. *Science*, *330*, 952–954. https://doi.org/10.1126/science.1196285

Rubino, M., D'Onofrio, A., Seki, O., & Bendle, J. A. (2015). Ice-core records of biomass burning. *The Anthropocene Review*, *3*, 140–162. https://doi.org/10.1177/2053019615605117

Rubino, M., Etheridge, D. M., Trudinger, C. M., Allison, C. E., Battle, M. O., Langenfelds, R. L., et al. (2013). A revised 1000-year atmospheric $\delta^{13}C$-CO_2 record from Law Dome and South Pole, Antarctica. *Journal of Geophysical Research: Atmospheres*, *118*, 8482–8499. https://doi.org/10.1002/jgrd.50668

Rudolph, J. (1995). The tropospheric distribution and budget of ethane. *Journal of Geophysical Research*, *100*, 11,369–11,381. https://doi.org/10.1029/95JD00693

Sachs, J. P., Sachse, D., Smittenberg, R. H., Zhang, Z., Battisti, D. S., & Golubic, S. (2009). Southward movement of the Pacific Intertropical Convergence Zone AD 1400–1850. *Nature Geoscience*, *2*, 519–525. https://doi.org/10.1038/ngeo554

Sapart, C. J., Monteil, G., Prokopiou, M., van de Wal, R. S. W., Kaplan, J. O., Sperlich, P., et al. (2012). Natural and anthropogenic variations in methane sources during the past two millennia. *Nature*, *490*, 85–88. https://doi.org/10.1038/nature11461

Schwietzke, S., Sherwood, O. A., Bruhwiler, L. M. P., Miller, J. B., Etiope, G., Dlugokencky, E. J., et al. (2016). Upward revision of global fossil fuel methane emissions based on isotope database. *Nature*, *538*, 88–91. https://doi.org/10.1038/nature19797

Simoneit, B. R. T., Schauer, J. J., Nolte, C. G., Oros, D. R., Elias, V. O., Fraser, M. P., et al. (1999). Levoglucosan, a tracer for cellulose in biomass burning and atmospheric particles. *Atmospheric Environment*, *33*(2), 173–182. https://doi.org/10.1016/s1352-2310(98)00145-9

Simpson, I. J., Sulbaek Andersen, M. P., Meinardi, S., Bruhwiler, L., Blake, N. J., Helmig, D., et al. (2012). Long-term decline of global atmospheric ethane concentrations and implications for methane. *Nature*, *488*, 490–494. https://doi.org/10.1038/nature11342

Solomon, S., Qin, D., Manning, M., Chen, Z., Marquis, M., Averyt, K., et al. (2007). Observations: Surface and Atmospheric Climate Change. In *Contribution of Working Group I to the Fourth Assessment Report of the Intergovernmental Panel on Climate Change* (pp. 235–337). Cambridge, United Kingdom and New York, NY, USA: Cambridge University Press. Retrieved from https://www.ipcc.ch/report/ar4/wg1/

Sowers, T. (2010). Atmospheric methane isotope records covering the Holocene period. *Quaternary Science Reviews*, *29*, 213–221. https://doi.org/10.1016/j.quascirev.2009.05.023

Stein, O., & Rudolph, J. (2007). Modeling and interpretation of stable carbon isotope ratios of ethane in global chemical transport models. *Journal of Geophysical Research*, *112*, D14308. https://doi.org/10.1029/2006JD008062

Tzompa-Sosa, Z. A., Mahieu, E., Franco, B., Keller, C. A., Turner, A. J., Helmig, D., et al. (2017). Revisiting global fossil fuel and biofuel emissions of ethane. *Journal of Geophysical Research: Atmospheres*, *122*, 2493–2512. https://doi.org/10.1002/2016JD025767

van Aardenne, J. A., Dentener, F. J., Olivier, J. G. J., Klein Goldewijk, C. G. M., & Lelieveld, J. (2001). A 1° × 1° resolution data set of historical anthropogenic trace gas emissions for the period 1890–1990. *Global Biogeochemical Cycles*, *15*, 909–928. https://doi.org/10.1029/2000GB001265

van der Werf, G. R., Peters, W., van Leeuwen, T. T., & Giglio, L. (2013). What could have caused pre-industrial biomass burning emissions to exceed current rates? *Climate of the Past*, *9*, 289–306. https://doi.org/10.5194/cp-9-289-2013

van der Werf, G. R., Randerson, J. T., Giglio, L., Collatz, G. J., Kasibhatla, P. S., & Arellano, F. J. (2006). Interannual variability in global biomass burning emissions from 1997 to 2004. *Atmospheric Chemistry and Physics*, *6*, 3175–3226. https://doi.org/10.5194/acpd-6-3175-2006

van der Werf, G. R., Randerson, J. T., Giglio, L., Collatz, G. J., Mu, M., Kasibhatla, P. S., et al. (2010). Global fire emissions and the contribution of deforestation, savanna, forest, agricultural, and peat fires (1997–2009). *Atmospheric Chemistry and Physics*, *10*, 11,707–11,735. https://doi.org/10.5194/acp-10-11707-2010

van der Werf, G. R., Randerson, J. T., Giglio, L., van Leeuwen, T. T., Chen, Y., Rogers, B. M., et al. (2017). Global fire emissions estimates during 1997–2016. *Earth System Science Data*, *9*, 697–720. https://doi.org/10.5194/essd-9-697-2017

van Marle, M. J. E., Kloster, S., Magi, B. I., Marlon, J. R., Daniau, A. L., Field, R. D., et al. (2017). Historic global biomass burning emissions for CMIP6 (BB4CMIP) based on merging satellite observations with proxies and fire models (1750–2015). *Geoscientific Model Development*, *10*, 3329–3357. https://doi.org/10.5194/gmd-10-3329-2017

Vuille, M., Burns, S. J., Taylor, B. L., Cruz, F. W., Bird, B. W., Abbott, M. B., et al. (2012). A review of the South American monsoon history as recorded in stable isotopic proxies over the past two millennia. *Climate of the Past*, *8*, 1309–1321. https://doi.org/10.5194/cp-8-1309-2012

Wang, X., Jacob, D. J., Eastham, S. D., Sulprizio, M. P., Zhu, L., Chen, Q., et al. (2019). The role of chlorine in global tropospheric chemistry. *Atmospheric Chemistry and Physics*, *19*, 3981–4003. https://doi.org/10.5194/acp-19-3981-2019

Wang, Z., Chappellaz, J., Park, K., & Mak, J. E. (2010). Large variations in southern hemisphere biomass burning during the last 650 years. *Science*, *330*, 1663–1666. https://doi.org/10.1126/science.1197257

Whitby, R. A., & Altwicker, E. R. (1978). Acetylene in the atmosphere: Sources, representative ambient concentrations and ratios to other hydrocarbons. *Atmospheric Environment*, *12*, 1289–1296. https://doi.org/10.1016/0004-6981(78)90067-7

Xiao, Y., Jacob, D. J., & Turquety, S. (2007). Atmospheric acetylene and its relationship with CO as an indicator of air mass age. *Journal of Geophysical Research*, *112*, D12305. https://doi.org/10.1029/2006JD008268

Xiao, Y., Logan, J. A., Jacob, D. J., Hudman, R. C., Yantosca, R., & Blake, D. R. (2008). Global budget of ethane and regional constraints on U.S. sources. *Journal of Geophysical Research*, *113*, D21306. https://doi.org/10.1029/2007JD009415

Yevich, R., & Logan, J. A. (2003). An assessment of biofuel use and burning of agricultural waste in the developing world. *Global Biogeochemical Cycles*, *17*(4), 1095. https://doi.org/10.1029/2002GB001952

Reference From the Supporting Information

Sander, S. P., Ravishankara, A. R., Golden, D. M., Kolb, C. E., Kurylo, M. J., Molina, M. J., et al. (2006). *Chemical kinetics and photochemical data for use in atmospheric studies, evaluation no. 15*. Pasadena: JPL publication 06-2, jet Propulsion Laboratory. http://jpldataeval.jpl.nasa.gov